Fermi National Accelerator Laboratory

FERMILAB-Conf-96/447-E
DØ

Studies of QCD at the Tevatron with the DØ Detector

Ransom W. Stephens
For the DØ Collaboration

University of Texas at Arlington
USA

Fermi National Accelerator Laboratory
P.O. Box 500, Batavia, Illinois 60510

December 1996

Presented at the *XI International Workshop on High Energy Physics and Quantum Field Theory -QFTHEP96*, Sankt - Petersburg, Russia, September 12-18, 1996

Disclaimer

Distribution

Studies of QCD at the Tevatron with the DØ Detector

Ransom W. Stephens
For the DØ Collaboration
University of Texas at Arlington, USA

Abstract

QCD studies at Fermilab's Tevatron encompass a rich variety of topics. We present some of the latest results from the DØ experiment including probes of the standard model given by the inclusive jet cross section, the dijet invariant mass spectrum and several studies with direct photons. To complement these probes, we also present new results from precision examinations of the color interactions including studies of color coherence and jet azimuthal decorrelation.

1 Introduction

We present here several QCD analyses, some of which are still preliminary. We begin with a short discussion of the DØ experiment followed by a review of hadronic jet physics at $p\bar{p}$ colliders focusing on the role of hadronic calorimetry. The order in which I present the analyses loosely follows powers of α_s in perturbation theory. Starting with single inclusive jets, dijets and direct photons, then turning to analyses that require non-perturbative calculations including color coherence and jet azimuthal decorrelation.

My approach is to present QCD results as a test of QCD predictive power and as a probe for new phenomena with a background predicted by QCD. I attempt to give these perspectives as separate sides of the same coin.

2 Jet Physics With the DØ Detector

The DØ Collaboration is composed of more than 450 physicists from more than 48 institutions in ten countries. Over the past few years of Tevatron running, Run 1a and 1b, we have accumulated roughly 100 pb^{-1} of data. The detector is well described elsewhere [1]. I wish to point out here that the hadronic calorimetry extends out to pseudorapidity, $\eta = -\log\tan\theta/2$, of $|\eta| < 4.2$, with the excellent single hadron response: $0.5/\sqrt{E} + 0.004$ GeV. The electromagnetic calorimetry also extends to $|\eta| < 4.2$, but with a gap in the region $0.9 < |\eta| < 1.4$ where there is an excess of steel from the cryostat housing. The single electron response is $0.15/\sqrt{E} + 0.003$ GeV. The calorimeter is segmented into projective towers of size $\Delta\eta \times \Delta\phi = 0.1 \times 0.1$ and, in the central region ($|\eta| < 0.5$), is seven hadronic interaction lengthes thick.

Jet events are recorded if they pass a single jet trigger. Since the cross section for low transverse energy (E_T) jet production in $p\bar{p}$ collisions is huge and since our limit for recording events is 2 Hz, there are four separate triggers with separate jet E_T thresholds. Each of the triggers is tuned to contribute a managable fraction of the data. For example, the trigger with threshold $E_T > 30$ GeV was prescaled to contribute just 0.4 pb^{-1} whereas the highest E_T trigger with threshold $E_T > 115$ GeV was not prescaled at all, that is, every event that fired this trigger was recorded, yielding 91 pb^{-1}. The trigger thresholds and data recorded by the intermediate E_T triggers were: $E_T > 50$ GeV with 4.6 pb^{-1} and $E_T > 85$ GeV with 52 pb^{-1}.

Jets are formed from an initial colored parton showering through multiple soft gluon radiation, fragmentation, followed by the formation of bound states, hadronization. Jets are observed through the measurement of energy depositions in the electromagnetic and hadronic calorimeters. Many of the hadrons decay before they reach the calorimeter, thus jets may also contain photons from π^0 and η decays, and electrons, muons and their neutrinos from weak decays of initial state partons, and short lived states.

To identify a jet from calorimeter showers, we use an iterative cone algorithm [2]. This algorithm requires a minimal E_T deposition in a single tower, $\Delta\eta \times \Delta\phi = 0.1 \times 0.1$, of 1 GeV. In most of the studies presented here we use a cone radius in $\eta - \phi$ space of $R = 0.7$. The E_T of a jet is defined to be the E_T sum of the towers within the cone. The E_T-weighted direction of the jet, (η, ϕ), are calculated and the center of the cone repositioned on this axis. The jet E_T and direction are recalculated until the direction is stable. When two jets are close together, they are merged into one if they share more than half their

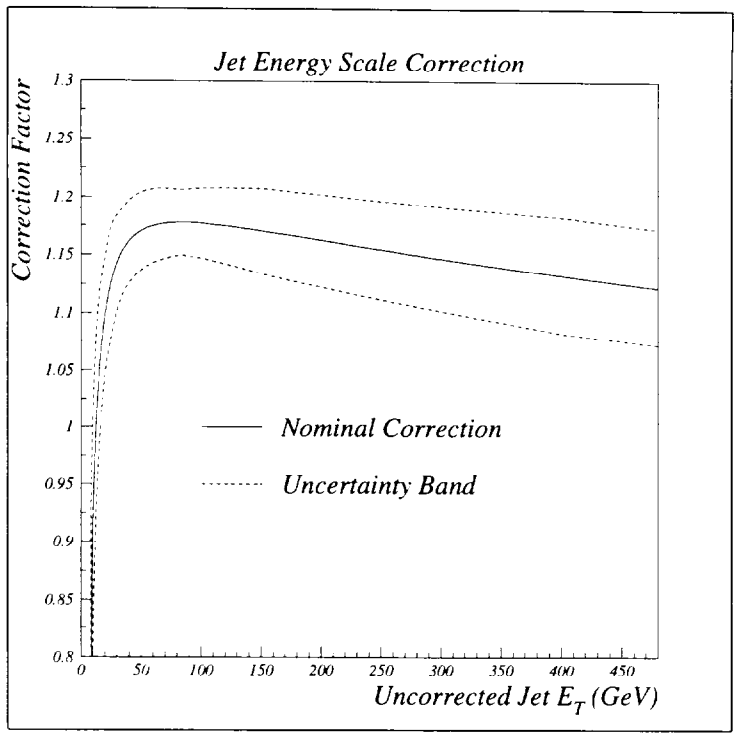

Figure 1: The jet energy scale correction factor as a function of uncorrected E_T. The dashed curves above and below the solid indicate the uncertainty.

E_T; otherwise they are split into two. A variety of quality and fiducial cuts are applied, resulting in jets with less than two percent contamination and efficiencies of about 95%.

There are many sources of nonlinearity in the E_T reconstruction of a jet. As the E_T of a jet increases, the E_T of the hardest particle increases roughly as $\log E_T$. Thus the number of particles in the jet increases rapidly with E_T, resulting in jets of many low E_T particles. The primary sources of nonlinearity in jet reconstruction are: very low E_T particles are absorbed in noninstrumented parts of the detector; the calorimeters don't precisely compensate (i.e., energy deposited by hadrons in the electromagnetic calorimetry doesn't match the energy deposited in the hadronic calorimetry); energy is lost outside the jet cone; the debris of the intial state proton and anti-proton (i.e., the underlying event), randomly populate the detector overlapping with jets; and, energy is lost to undetected neutrinos from particle decays within jets. The determination of the jet energy scale, constitutes a difficult physics analysis in its own right, the science of correcting for all these effects. The energy scale correction corrects jets "back to the parton level." I put this phrase in quotations because it is fundamentally impossible. Partons are colored objects and we observed color-singlets in our detector. Thus the initial state partons in an event interact with each other and we cannot in principle reconstruct them. Ironically we are saved from this by the fact that hadronic calorimetry is not a precise measuring device. The errors in jet reconstruction greatly outweigh the uncertainty introduced by initial state parton interactions. The best that a state of the art hadronic calorimetry can do is a resolution of $0.5/\sqrt{E_T}$ for single particles in nice parts of the detector! We are familiar with the analogy: to study matter by smashing a proton into an anti-proton is like studying fine Swiss watches by smashing them together and looking at the broken pieces. I propose an extension of this analogy: to study the pieces with a hadronic calorimeter is akin to looking at them with a hammer. In short, hadronic calorimetry is a blunt instrument.

In Fig. 1 we present the correction factor as a function of the uncorrected jet E_T with the uncertainty band. This jet energy scale correction will be our dominant source of systematic error in the analyses which follow.

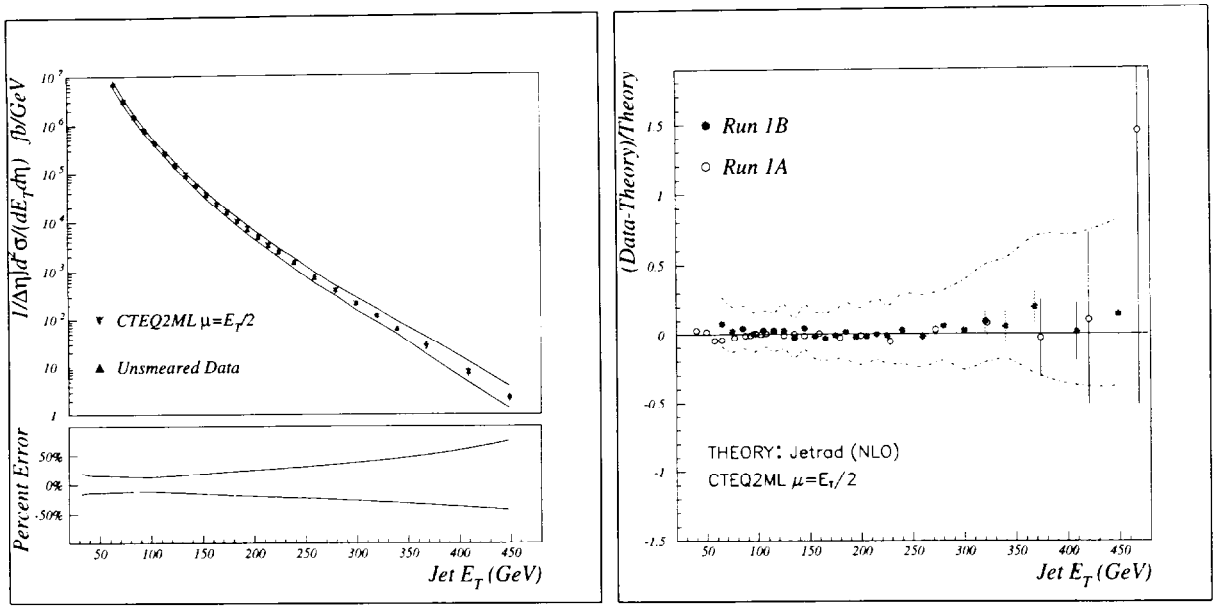

Figure 2: Measurement of the single jet inclusive cross section, (a) the single jet inclusive cross section with systematic error given below, (b) the fractional difference between the DØ measurements of the single jet inclusive cross section and NLO QCD with the CTEQ2ML PDF and renormalizations scale, μ, of half the E_T of the hardest jet in the event. The measurement from Run 1a (1b) of the Tevatron is given with open (solid) circles

3 Single Jet Analyses

Collider detectors directly observe electrons, muons, photons and jets. Since the cross section for jet production is much larger than that for any of the other observed particles, it's easy to argue that the single jet inclusive cross section is the most basic measurement to be performed at a $p\bar{p}$ collider. In this analysis we present the differential cross section for central jets as a function of the jet E_T.

From the point of view of a test of QCD, the leading order QCD prediction carries a theoretical uncertainty of as much as 50%; but just one order higher, next-to-leading order (NLO) QCD reduces this to about 20%. Hence this measurement can probe the theory with some sensitivity. Other than the effects of higher orders, the uncertainty in the theory is confined to four choices: the parton distribution function (PDF), the factorization scale μ_F, the renormalization scale μ_R and the parton shower model. In the following we set $\mu_F = \mu_R = \mu$.

From the point of view of a search for new phenomena, a signal for quark compositeness is the increase in the single jet cross section at an E_T threshold.

In this analysis we choose events with all and only good jets by subjecting candidates to criteria for eliminating fake jets and poorly reconstructed jets. The inclusive measurement is for jets in the central region, $|\eta| < 0.5$, of the detector where the efficiency and energy are well understood. To combine the data from separate triggers, we equate the cross sections measured from two triggers neighboring in E_T threshold where both triggers are efficient. The absolute normalization is then fixed by the highest E_T trigger threshold which is not prescaled, i.e., by jets with $E_T > 170$ GeV.

We choose the CTEQ2ML PDF [3] — the spread of predictions using a variety of PDFs is about 20%; and renormalization scale, $\mu = E_T^{\max}/2$ where $E_T^{\max}$ is the transverse energy of the hardest jet in a given event. The NLO QCD prediction, with these choices, is performed by the JETRAD Monte Carlo [4] simulation.

The single jet inclusive cross section is presented in Fig. 2(a). The systematic error, which is dominated by the jet energy scale correction, is also shown. Comparison with the NLO QCD prediction is simplified by considering the fractional difference between the measurement and the theory, Fig. 2(b).

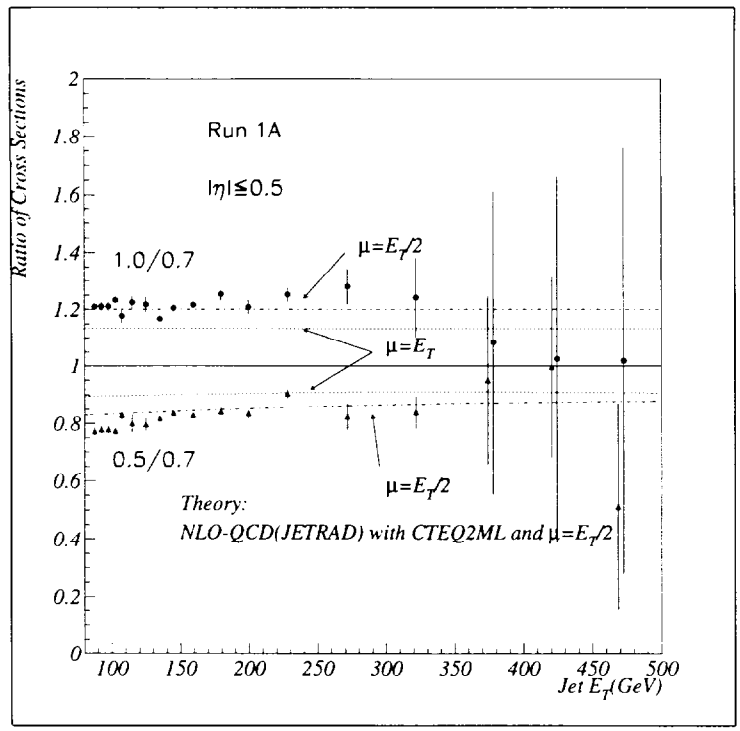

Figure 3: The ratios of cross sections for different cone sizes compared to NLO QCD predictions with different renormalization scales.

With this choice of PDF and μ, the data and theory agree in absolute normalization. Early this year, the CDF collaboration released a preprint [5] including their measurement of the single jet inclusive cross section using the MRSD0′ PDF [6] that they said was "significantly higher than NLO QCD" above $E_T = 200$ GeV and which demands "a reevaluation of theoretical predictions and uncertainties within and beyond the standard model." Since our measurement and the CDF measurement were performed with slightly different jet reconstruction algorithms over a different range of pseudorapidity, a direct comparison of the two measurements is not straightforward. The comparison performed by Lai and Tung for a variety of different PDFs [7] demonstrated that the DØ and CDF measurements are consistent and that the deviation from the NLO QCD prediction reported by CDF is well within the theoretical error. In the evolution from preprint to publication, CDF removed the above statement about reevaluation of the standard model [8].

By studying the ratios of single jet inclusive cross sections measured with different cone sizes we eliminate most of the theoretical error from the choice of PDF and parton clustering. This leaves a measurement sensitive to the renormalization scale, μ. In Fig. 3 we present the cross section ratios for $R = 1.0/R = 0.7$ and $R = 0.5/R = 0.7$ with theoretical predictions for the two choices: $\mu = E_T^{\max}$ and $\mu = E_T^{\max}/2$. The data clearly indicates a preference for $\mu = E_T^{\max}/2$.

4 Dijet Analyses

Another test of NLO QCD is the measurement of the dijet cross section as a function of the dijet invariant mass. This analysis has the ingredients for a truely model independent new phenomena probe: the dijet invariant mass spectrum where we may hope to observe a resonant structure peaking above the smooth continuous background shape.

We consider two separate regions of the detector for the jets in this study: (1) both central jets, $|\eta_{1,2}| < 0.5$, and (2) less central jets, $|\eta_{1,2}| < 1.0$ but with their separation restricted, $\Delta\eta_{1,2} < 1.6$.

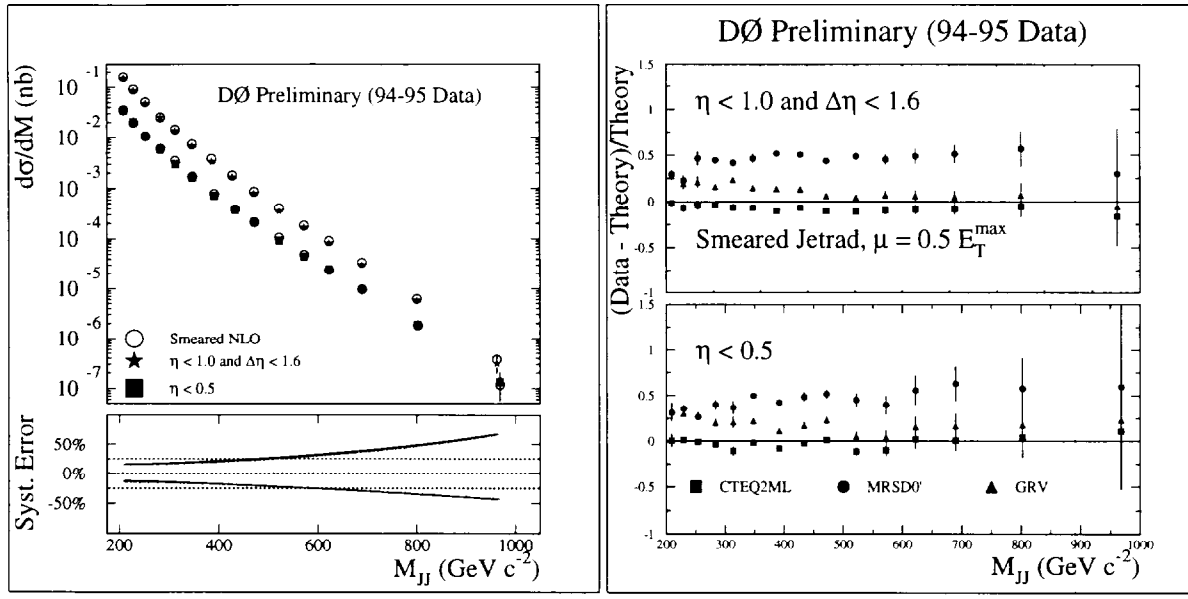

Figure 4: The PRELIMINARY dijet cross section, (a) $d\sigma/dM_{jj}$, for two separate η regions compared with NLO QCD using CTEQ2ML PDF and $\mu = E_T^{\max}/2$ with systematic error given in the lower plot, (b) the fractional difference between the dijet cross section and NLO QCD with three separate PDF choices.

Assuming that individual jets are massless, the dijet invariant mass is given by

$$M_{jj}^2 = 2E_T^{(1)}E_T^{(2)}[\cosh\Delta\eta - \cos\Delta\phi],$$

where $E_T^{(1)}$ and $E_T^{(2)}$ are the two hardest jets in the event. The single jet triggers are used in M_{jj} ranges where the efficiencies are close to 100%. Events are weighted according to their trigger by requiring that the cross sections be the same in the kinematic region where pairs of triggers overlap — the highest E_T trigger is not prescaled and so is intrinsically normalized for $M_{jj} > 270$ GeV. We show the cross section in Fig. 4(a) with NLO prediction performed by JETRAD with the CTEQ2ML PDF and $\mu = E_T^{\max}/2$. The systematic error varies from about 13% at $M_{jj} = 200$ GeV to about 55% at 950 GeV.

It is interesting to compare this measurement with predictions using other PDFs: MRSD0′ and GRV [9], Fig. 4(b). The data clearly follow the CTEQ2ML PDF more closely than the other two shown — note that this only implies that CTEQ2ML is closer to the truth than the others if there is no physical process beyond QCD in these measurements.

From the perspective of a new phenomena search, Fig. 5(a) shows the invariant mass spectrum, M_{jj}. The smooth curve comes from a fit of the smeared NLO QCD prediction to the data. Since there is no indication of any deviation from the smooth background shape, we set upper limits on excited quark masses, M_{q^*}, in Fig. 5(b). These limits are set by fitting the number of events in each bin: $N_{\text{fit}} = p_1 \times$ (NLO QCD shape) $+ N_R \times$ (excited quark signal shape).

The dijet angular distribution features little dependence on the PDF choice. Consider the angle, θ^*, between an initial parton and a final parton in the center of mass frame of a $2 \to 2$ process. At leading order this distribution is described by the Rutherford prediction; at NLO it's more complicated. Here, we consider a variable χ, related to θ^* by

$$\chi = \frac{1+\cos\theta^*}{1-\cos\theta^*} = e^{|\eta_1-\eta_2|}$$

because it's easy to measure.

Since this is a geometric distribution, we do not need to worry about the jet energy scale so we can reach farther in η: $\eta_{1,2} < 3.0$. For large masses, $M_{jj} > 550$ GeV, we present the χ distribution along

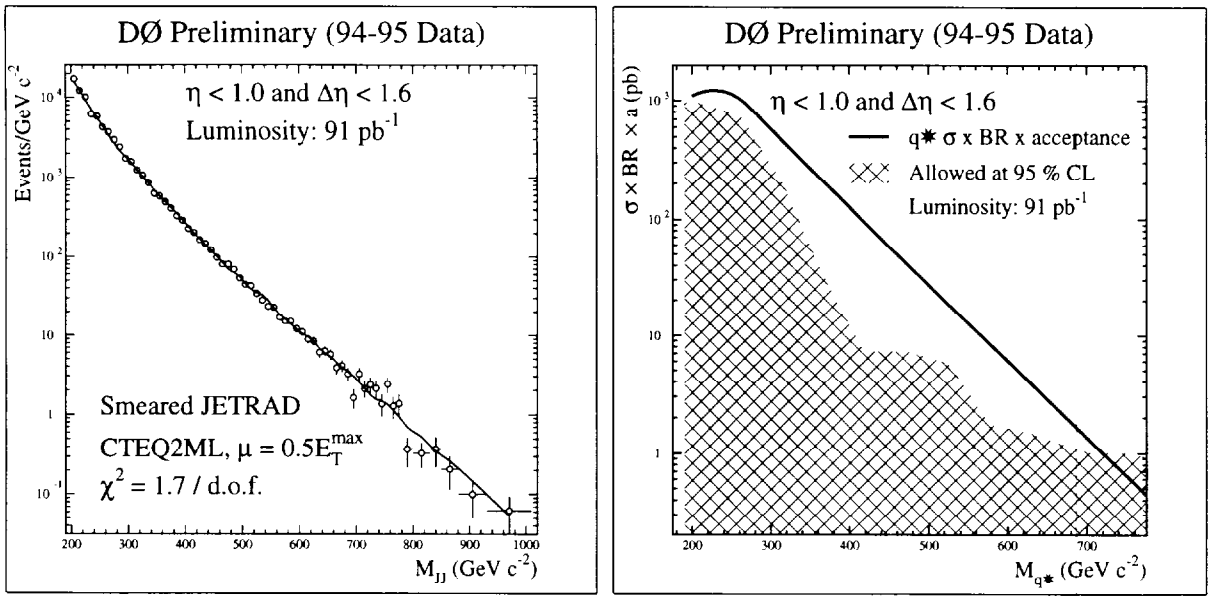

Figure 5: (a) The PRELIMINARY dijet invariant mass spectrum, the smooth curve is a fit of the NLO QCD prediction to the data and (b) the PRELIMINARY 95% confidence level upper limit on excited quark mass derived from the dijet analysis.

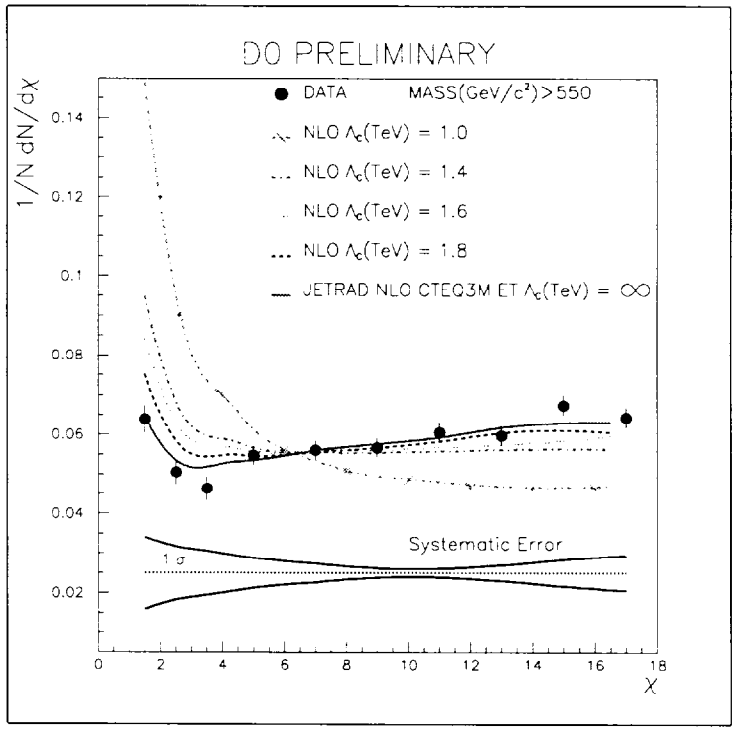

Figure 6: The PRELIMINARY dijet angular distribution, χ, including composite quark predictions with various contact terms and our systematic uncertainty.

with a NLO QCD prediction and composite quark predictions for a variety of different contact terms, Λ_C, in Fig 6. The composite quark predictions are made by multiplying the leading order prediction of the PAPAGENO Monte Carlo [10] with the ratio of the NLO and LO JETRAD predictions to extract a NLO composite prediction. The data closely follow the NLO QCD prediction.

5 Direct Photon Analyses

The detection of photons does not have the large experimental uncertainty associated with jet measurement; and since they are gauge bosons similar to gluons, events with jets and photons probe the gluon distributions of colliding hadrons. Conceptually, one can simply replace a gluon leg in a Feynman diagram with a photon.

We present three separate direct photon analyses here: the inclusive single photon cross section [11], the angular distribution of photons in γ+jet events and photon-jet rapidity correlations.

In the DØ detector we have effective electro-magnetic calorimetry for $|\eta| < 0.9$ and $1.6 < |\eta| < 2.5$. Identification of photons is essentially the identification of electromagnetic (EM) calorimeter showers unassociated with charged tracks. Specifically, we require that: (1) the EM energy fraction be 0.96 of the total; (2) there be no charged tracks within a region of roughly $\Delta\eta \times \Delta\phi = 0.2 \times 0.2$ centered on the candidate photon; (3) the shower shape be consistent with test beam electrons; and, (4) an isolation requirement, $E_T^{R=0.4} - E_T^{R=0.2} < 2$ GeV, where E_T^R is the E_T within a cone of radius R. These criteria yield efficiencies of $85 \pm 1\%$ for $|\eta| < 0.9$ and $61 \pm 3\%$ for $1.6 < |\eta| < 2.5$. To reject backgrounds from $W \rightarrow e\nu$, where the e is mistaken for a γ, we require that the missing transverse energy in the events be less than 20 GeV.

The background is dominated by the tiny fraction of the total cross section of jets that hadronize into only particles with electromagnetic decays, like $\pi^0 \rightarrow \gamma\gamma$. Since the total jet cross section is so huge, these processes yield a substantial background. To calculate the photon purity P we use the fact that these fluctuating jets appear in the detector as overlapping photons. Thus the probability of a conversion in the first EM layer of the calorimeter is at least twice that of a single photon. If we let E_1 be the energy in the first EM layer, then we consider $\log E_1/E_{\rm total}$. We extract the purity by fitting the $\log E_1/E_{\rm total}$ distribution to a sum of Monte Carlo simulations of the single photon signal and the π^0 and η backgrounds, as shown in Fig. 7(a). These fits are performed separately in E_T^γ intervals and η regions. The purity as a function of E_T^γ is shown for the two η regions in Fig. 7(b). We paramaterize the purity as $P = 1 - e^{-(a+bE_T^\gamma)}$ where a and b are the fit parameters. The systematic error is dominated by differences in data compared to Monte Carlo.

The inclusive single photon cross section for the two η regions is given in Fig. 8. The NLO QCD prediction is provided by Baer, Ohnemus and Owens [12] with the CTEQ2M PDF and $\mu = E_T^\gamma$. The fractional difference between the measurement and the theory is given in Fig. 9(a); Fig. 9(b) shows the ratio of the cross sections for the two η regions, where the uncertainty in luminosity cancels. In figures 9 (a) and (b) there is a considerable difference between the theory and measurement for $E_T^\gamma < 30$ GeV. While this is the kinematic region where the systematic error due to split neutral meson clusters is largest, as indicated by the shaded area below the data, similar effects have been observed by other experiments [13] and a theoretical explanation including additional initial state parton showering in NLO QCD has been proposed [14].

Since it is not sensitive to the PDF choice in NLO QCD, measurement of the angular distribution of direct photons in $\gamma + jet$ events is a sensitive probe of the matrix elements of the theory. For this measurement we select events with a direct photon and at least one hadronic jet. All hadronic jets in an event are combined into one object that includes NLO and higher order corrections, thereby retaining the simplicity of the $2 \rightarrow 2$ process. We require $E_T^\gamma > 30$ GeV; $|\eta_\gamma| < 0.9$; $|\eta_{jet}| < 3.0$; and, missing-$E_T < 0.3E_T^\gamma$. The distribution of the photon decay angle, θ^* is given by $\cos\theta^* = \tanh\eta^*$ where $\eta^* = 0.5(\eta_\gamma - \eta_{jet})$.

The shape of the background was obtained from a pure sample of jets and then subtracted using the purity as the relative normalization. The resulting distribution is presented in Fig. 10 which also includes the CDF measurement [15] and NLO QCD prediction [12]. Our measurement is consistent with, though systematically lower than, the CDF measurement and in accord with the theoretical prediction.

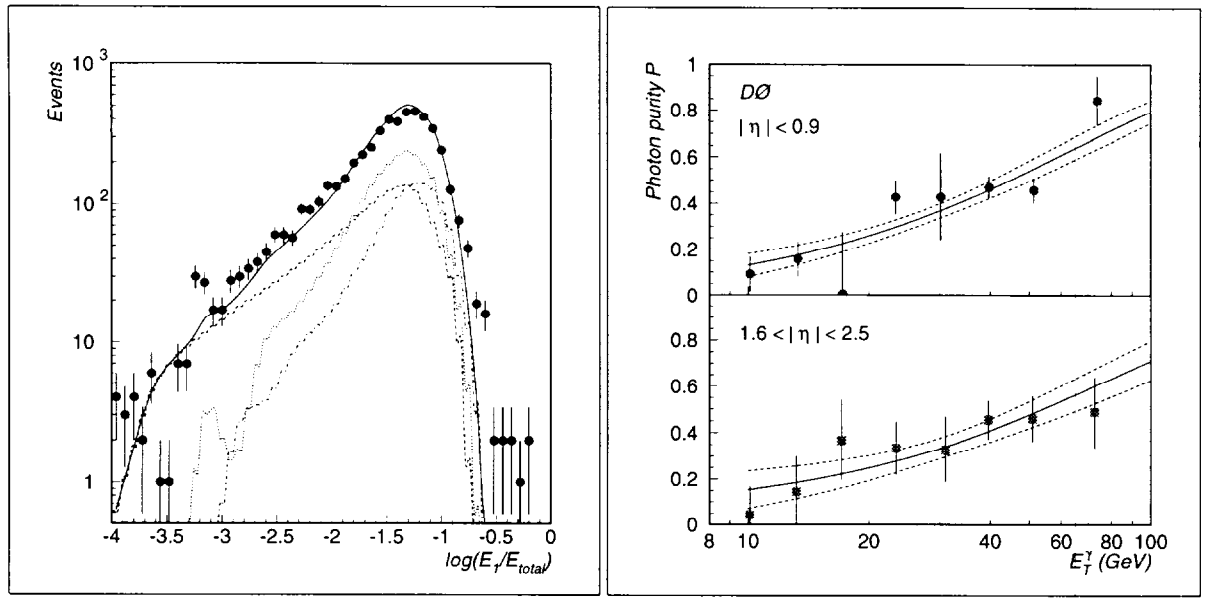

Figure 7: (a) The $\log E_1/E_{\rm total}$ distribution for Monte Carlo simulations of photons (dashed), π^0s (dotted) and ηs (dot-dashed) with the data (solid points with statistical error bars); (b) the photon purity as a function of E_T^γ, the curve is a fit to the measured purity, the dashed curves indicate the error of the fit.

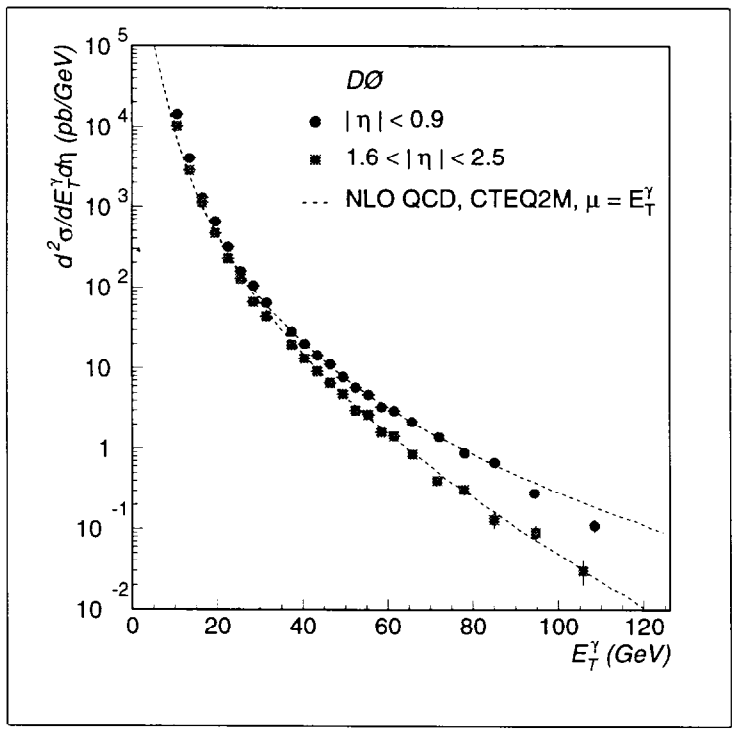

Figure 8: The inclusive single photon cross section for the central ($|\eta| < 0.9$) and forward ($1.6 < |\eta| < 2.5$) regions of the detector. The curves are NLO QCD corrections with the CTEQ2M PDF and $\mu = E_T^\gamma$.

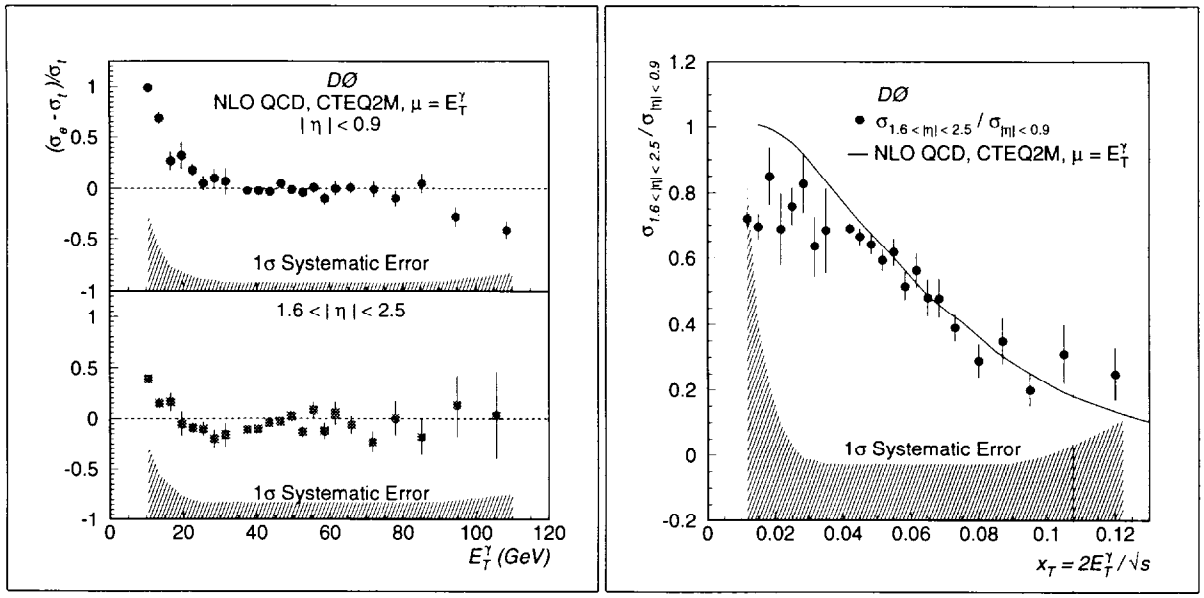

Figure 9: (a) The fractional difference between the measured and theoretical single inclusive photon cross sections for both central and forward photons, (b) the ratio of the forward to central cross sections with the NLO QCD prediction. The NLO QCD predictions use the CTEQ2M PDF and $\mu = E_T^\gamma$.

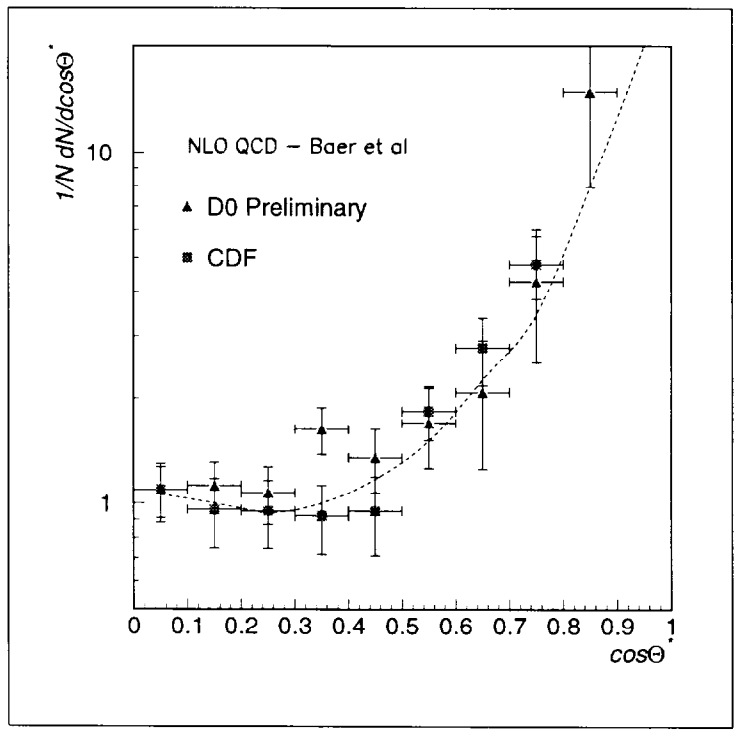

Figure 10: The PRELIMINARY angular distribution of gamma plus jet events for $|\eta| < 0.9$. The triangles represent the DØ measurement and the squares represent the CDF measurement.

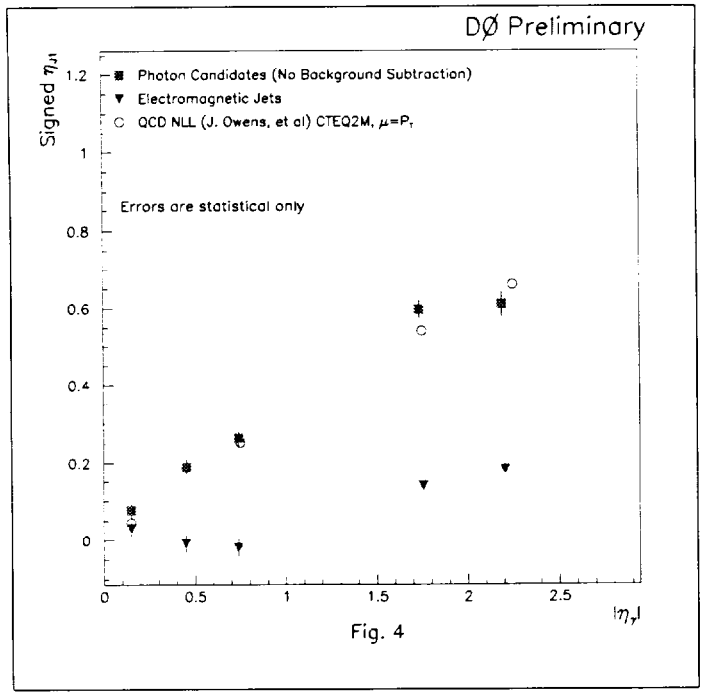

Figure 11: The PRELIMINARY measurement of the signed pseudorapidity of the highest E_T jet of an event, η_{j1} as a function of the photon pseudorapidity, $|\eta_\gamma|$. The sqaures are for photon candidates, the triangles for electromagnetic jets, a control sample, and the circles are a NLL QCD prediction using CTEQ2M PDFs and $\mu = E_T^\gamma$.

In the next analysis we compare the correlation of jets and photons in $\gamma + jets$ events with the correlation of the two highest E_T jets in multiple jet events. Direct photon production is dominated by qg scattering and multiple jets are dominated by gg and qq interactions. In the $gg/qq \rightarrow jets$ reaction, the partons in both the initial and final states can radiate gluons; whereas in the $qg \rightarrow \gamma + jets$ reaction the final state photon cannot radiate gluons. Thus, if we think of photons and gluons as generic gauge bosons, then in any Feynman diagram above leading order, there will always be more diagrams for a given number of jets in $gg/qq \rightarrow jets$ then there are for that number of gauge bosons (including the jets plus one photon) in $qg \rightarrow \gamma + jets$. Consequently, as we go to higher orders in perturbation theory, the $\gamma + jets$ final states retain more of the $2 \rightarrow 2$ identity of the leading order process, than do the multiple jet final states. Thus we expect larger correlation of η_{jet} and η_γ in $\gamma + jets$ events than $\eta_{jet}^{(1)}$ and $\eta_{jet}^{(2)}$ in multiple jet events.

In this PRELIMINARY analysis we consider the η_γ and η_{jet} distributions, expecting η_{jet} to follow η_γ. We accept both central, $|\eta_\gamma| < 0.9$, and forward, $1.5 < |\eta_\gamma| < 2.5$, photons with $E_T^\gamma > 45$ GeV. Since we cannot perform a statistical background subtraction in this analysis, we need greater photon purity. Thus we require $E_1/E_{total} < 1\%$ giving better than 75% photon purity. For a control sample we consider the distibution of η for multiple jet events selected to discriminate against photons — isolation > 2 GeV, $E_1/E_{total} > 1\%$, allowance of two or more tracks in front of an EM cluster, increased hadronic energy, non-photon-like shower shape — giving a sample dominated by jets with a large electromagnetic component: "electromagnetic jets." Figure 11 shows the signed pseudorapidity of the jet, η_{jet}, positive if in the same rapidity directon as the photon candidate and negative if opposite, as a function of $|\eta_\gamma|$. We observe a strong correlation in the $\gamma + jets$ sample that is well described by the QCD NLL theory [12]. The control sample of "electromagnetic" jets, mimicing fake photons, does not demonstrate the correlation.

6 Color Coherence

Color coherence results from interference of amplitudes for soft gluon radiation from partons during fragmentation [16]. This phenomenon links perturbative and non-perturbative QCD. The perturbative effect is angular ordering, and the non-perturbative effect is string fragmentation. Angular ordering requires that initial state partons are radiated with successively increasing angles with respect to the parent parton and final state partons radiate with successively decreasing angles. Angular ordering results in the suppression of soft gluon radiation in certain regions of phase space. String fragmentation describes the color connections that dictate the gross features of fragmentation. It is particularly interesting to ponder whether or not the footprint of color coherence can survive the hadronization process.

We present two separate approaches to investigating color coherence. In the first, we consider color links between the initial state beams and the softer jets in multiple jet events. In the second, using $W + jet$ events we compare energy depositions around the jet with those around the W boson.

First, our multiple jet analysis. We choose events with three or more jets and assemble the jets in order of decreasing E_T: $E_{T1} > E_{T2} > E_{T3}$. We require $E_{T1} > 115$ GeV and $E_T > 15$ GeV for at least two other jets in the event. Consider the angular distribution of the third jet about the second. Let β be the azimuthal angle of the third jet, in (η, ϕ) space, about the second, so that $\beta = 0$ and $\beta = \pi$ are in the same plane as the colliding beams and the second jet — we call this the event plane. We can write β as

$$\beta = \tan^{-1} \frac{\text{sign}(\eta_2)\Delta\phi}{\Delta\eta}$$

where $\Delta\phi = \phi_3 - \phi_2$ and $\Delta\eta = \eta_3 - \eta_2$. We look for jets in an annulus about the second jet of size $0.6 < R < \pi/2$. Color coherence predicts that soft jet emission will be enhanced near $\beta = 0, \pi$ (i.e., near the event plane) compared to $\beta = \pi/2, 3\pi/2$ (perpendicular to the event plane).

By comparing the distribution of the data with those of different Monte Carlo simulations some without any color coherence and some with different color coherence models, we can identify the effect in the data and indicate the accuracy of the various models. Figure 12 shows the ratio of the data and Monte Carlo β distributions for two separate η ranges. The figures on the left are for central jets $|\eta_2| < 0.7$, those on the right for more forward jets, $0.7 < |\eta_2| < 1.5$. In the two top sets of plots with Monte Carlo simulations, ISAJET 7.13 [17] and PYTHIA 5.7 [18], with color coherence turned off, it is apparent that the data exceeds the Monte Carlo near the event plane, $\beta \sim 0, \pi, 2\pi$, and is depleted perpendicular to the event plane, $\beta \sim \pi/2, 3\pi/2$. The third and fourth plots from the top both include color coherence, PYTHIA 5.7 and HERWIG 5.8 [19], and the bottom plot is the NLO QCD prediction provided by JETRAD. PYTHIA and HERWIG adequately predict the effect and, intriguingly, NLO QCD also accurately represents the data.

In the PRELIMINARY $W + jet$ analysis, we capitalize on the fact that the W is colorless and so any effect we see around a jet can be compared with that around the W. We require that the jet be in the central region of the detector, $|\eta| < 0.5$, and $W \to e\nu$ candidates are selected by requiring an electron with $E_T^e > 25$ GeV, event missing-$E_T > 25$ GeV and W rapidity restricted to $|y_W| < 0.5$. The W boson and jet were required to be in opposite ϕ hemispheres and, to retain the projectivity of the calorimeter towers, the event vertex was restricted to $|z_{\text{vtx}}| < 20$ cm.

Consider the azimuthal distribution of calorimeter towers, $\Delta\eta \times \Delta\phi = 0.1 \times 0.1$, with E_T deposits greater than 250 MeV in annuli about the jet and the W boson. That is, we use the same azimuthal angle definition, β, as in the multiple jet analysis, for energetic towers around the jet and W boson. Similar to the multiple jet case, color coherence predicts an enhancement in the number of energized towers around the jet in the regions $\beta \sim 0, \pi$ and a depletion for $\beta \sim \pi/2$, but no effect at all around the W boson. The ratio of the number of towers with $E_T > 250$ MeV in β bins around a jet to that around a W boson is given by N^{jet}/N^W. We compare the β distribution of this ratio with a control sample and with the PYTHIA Monte Carlo simulation without and with varying degrees of color coherence in Fig. 13. The control sample is composed of minimum bias data with fake jet and W boson locations randomly placed in each event, but weighted to reflect the η_{jet}, y_W and $\Delta\phi$ distributions in genuine $W + jet$ events. Figure 13(a) clearly demonstrates the color coherence signal in the $W + jet$ data with no detector related effect that could mimic the signal appearing in the control sample. In Fig. 13(b) we see the N^{jet}/N^W distributions for three separate PYTHIA simulations, one with both angular ordering and

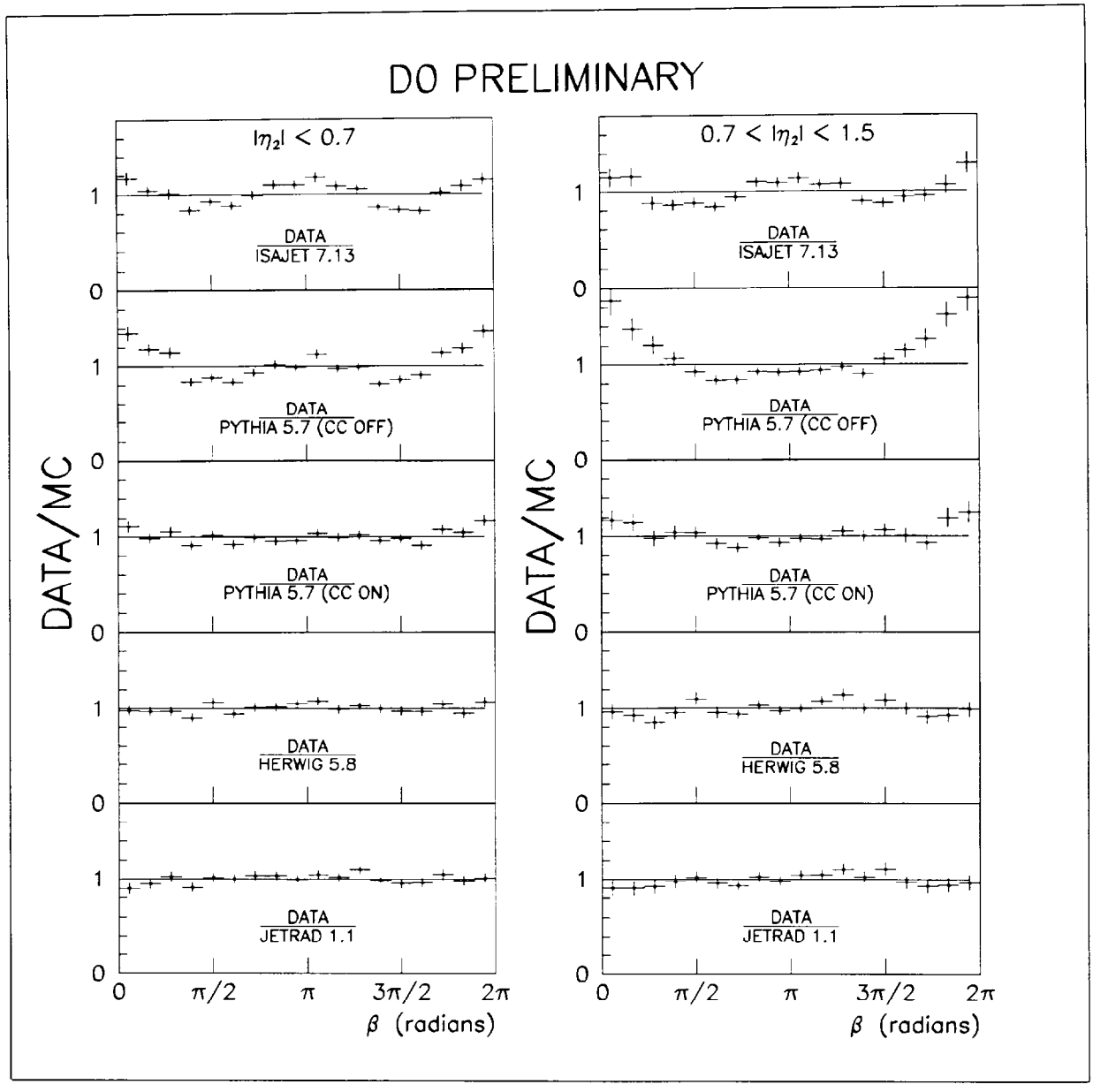

Figure 12: The PRELIMINARY ratio of data to Monte Carlo predictions of the third jet's azimuthal angle, β, about the second jet. The plots on the left are for $|\eta_2| < 0.7$, those on the right are for $0.7 < |\eta_2| < 1.5$. The Monte carlo models are labeled, the top two sets of plots do not include color coherence, the third and fourth from the top do include color coherence and the bottom set compare data with NLO QCD provided by JETRAD.

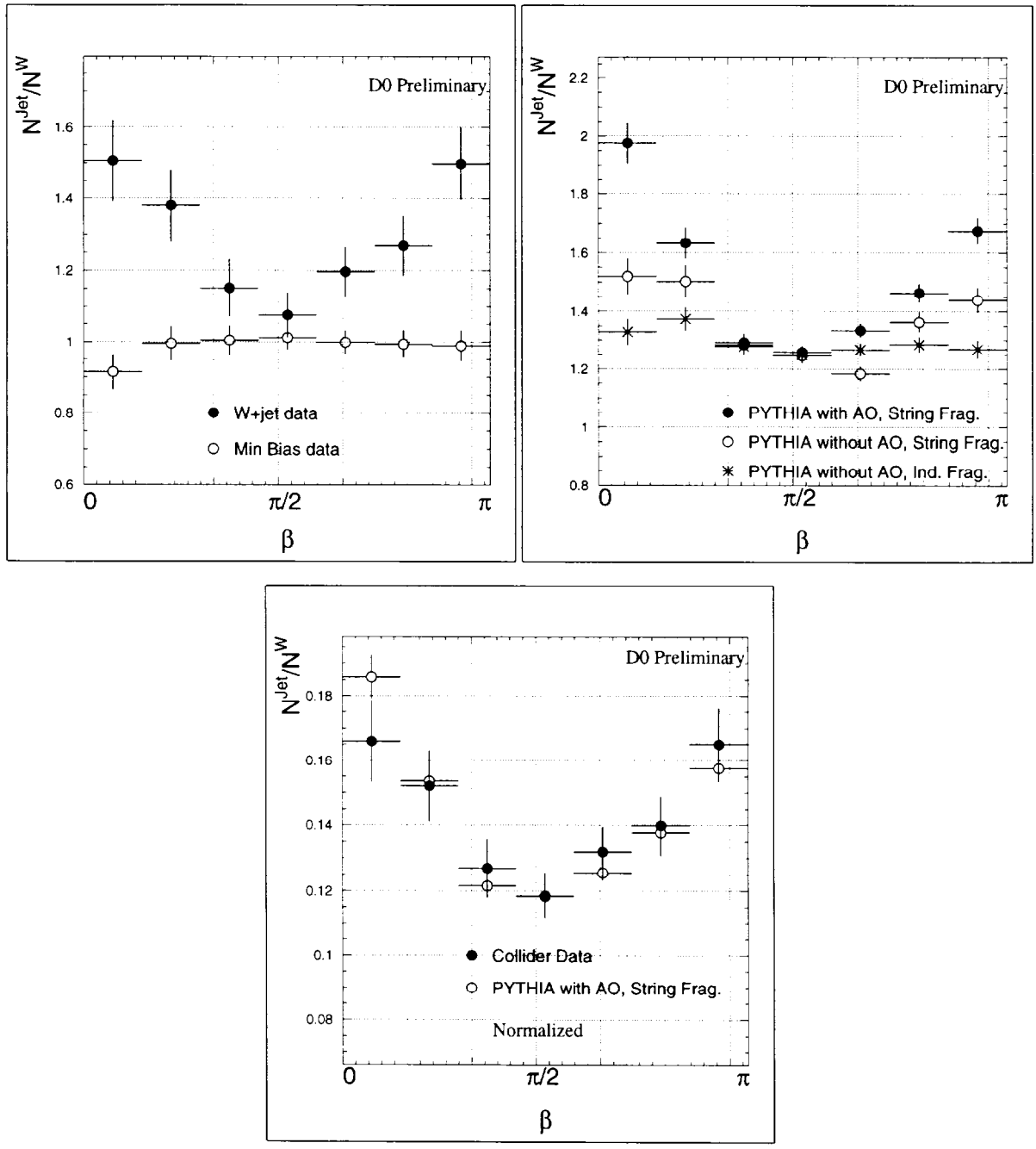

Figure 13: The PRELIMINARY $N^{\rm jet}/N^{W}$ vs β distributions for (a) the $W+jet$ data and control samples, (b) PYTHIA Monte Carlo simulations with and without color coherence and, (c) the $W+jet$ data and the Monte Carlo with full color coherence.

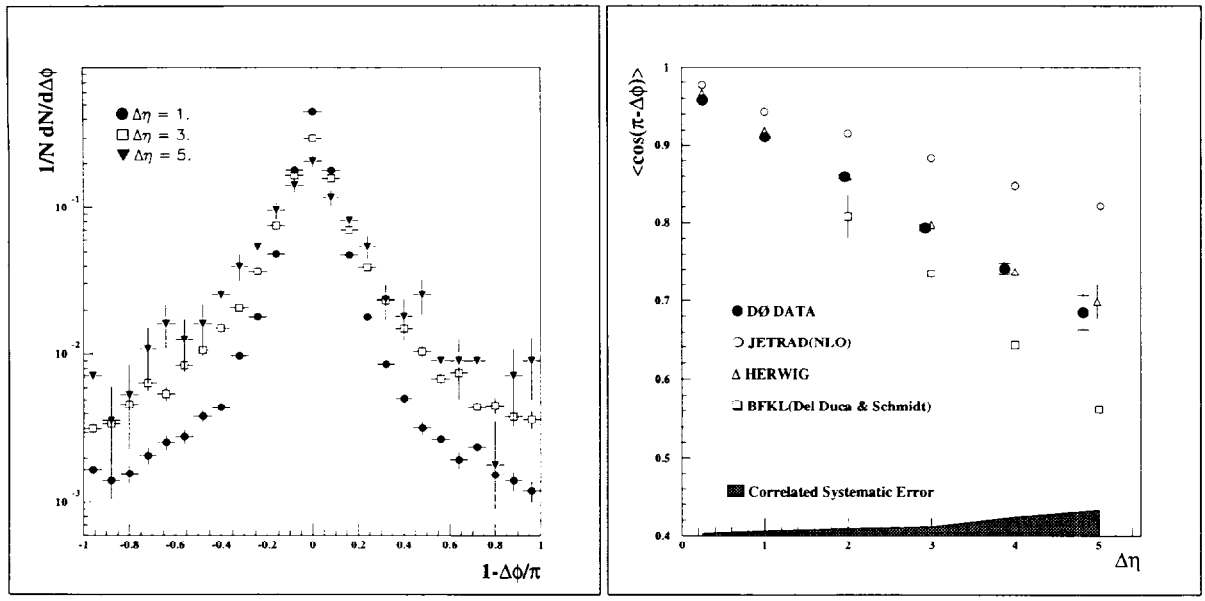

Figure 14: Demonstration of azimuthal decorrelation of jets widely separated in pseudorapidity, $\Delta\eta$, (a) the distribution of the azimuthal separation expressed as $1 - \Delta\phi/\pi$ for three regions of $\Delta\eta$, (b) measurement and predictions of decorrelation $\langle\cos(\pi - \Delta\phi)\rangle$ vs $\Delta\eta$.

string fragmentation, one with just string fragmentation and one with no color coherence at all. Figure 13(c) gives the $W + jet$ data plotted with the PYTHIA simulation with full color coherence. The Monte Carlo simulation, which includes both angular ordering and string fragmentation, accurately reproduces the data distribution much more effectively than the other simulations shown in Fig. 13(b).

7 Azimuthal Decorrelation in Multiple Jet Events

Beyond next-to-leading-order in perturbation theory, with final states including more than three jets, it is interesting to compare topological distributions of data with Monte Carlo simulations which include different theoretical and phenomenological approaches to handling non-perturbative effects. Excellent theoretical technology for resumming large logarithms in the cross section is provided by the BFKL formalism [20]. In multiple jet events with two jets widely separated in pseudorapidity, $\Delta\eta$, large logarithms of the type $\ln \hat{s}/Q^2$ appear in the cross section and must be resummed. These terms include leading powers in $\Delta\eta$ manifested as increased gluon radiation. Specifically, as $\Delta\eta$ grows we expect an increase in the production of low E_T jets causing a deviation from the LO QCD back-to-back dijet topology. Thus we look for a decorrelation in azimuthal angle, $\Delta\phi$, of two jets at extreme η. The results of our publication [21] have been extended to larger $\Delta\eta$ in the analysis presented here.

The data sample consists of events with at least two jets of $E_T > 20$ GeV. The jets are ordered in increasing η: $\eta_1 < \eta_2 < ... < \eta_N$. We study the distribution of $1 - \Delta\phi/\pi$, where $\Delta\phi = \phi_1 - \phi_N$, shown in Fig. 14(a) for three different $\Delta\eta$ ranges. As $\Delta\eta$ increases, the back-to-back correlation of the two jets diminishes — qualitative evidence of the theoretical prediction. Figure 14(b) gives $\langle\cos(\pi - \Delta\phi)\rangle$ vs $\Delta\eta$ for our data, NLO QCD prediction, HERWIG Monte Carlo simulation and the BFKL calculation of Del Duca and Schmidt [22]. The effect of decreasing correlation with increasing $\Delta\eta$ is quite pronounced. The BFKL calculation overestimates the effect, NLO QCD, as one might expect, underestimates it and HERWIG, with its phenomenological input, seems to demonstrate it quite accurately.

8 Conclusion

A wide variety of QCD analyses performed by the DØ Collaboration were presented from the perspective of tests of perturbative and non-perturbative theoretical approaches to the strong interactions and from the perspective of probing for new phenomena assuming QCD accurately describes the standard model background. We have seen that the model dependence of QCD — the need to choose parton distribution functions and renormalization/factorization scales — is still too large to nail down deviations from the standard model of the order of 20%. Further, the experimental limitations in measuring the energy of jets, especially given the technological limitations of hadronic calorimetry and the fundamental impossibility of correcting jets back to the parton level, make precision measurements of jet final states quite difficult.

Despite these difficulties, we have seen that perturbative QCD at NLO predicts the behavior observed by DØ quite accurately: in the the inclusive single jet cross section, the dijet cross section and invariant mass spectrum, the dijet angular distribution, the single photon inclusive cross section (with a hint of deviation from NLO QCD for $E_T^\gamma < 30$ GeV) and the direct photon angular distribution.

Analyses probing the non-perturbative realm of QCD have also been presented and are well described by phenomenological predictions provided by Monte Carlo simulation and, remarkably, by NLO QCD: photon-jet rapidity correlations and color coherence with multiple jet and with $W + jet$ events.

We presented the azimuthal decorrelation of jets widely separated in pseudorapidity which showed qualitative agreement with non-perturbative theoretical predictions and quantitative agreement with phenomenological Monte Carlo simulation.

I wish to emphasize that the results presented here are a subset of the work produced by The DØ Collaboration's young and prolific QCD group, to whom I am greatly indebted for the honor of presenting their fine work at this workshop.

References

[1] S. Abachi et al. (The DØ Collaboration), Nucl. Instr. Meth. A 338 (1994) 185.

[2] S.D. Ellis, J. Huth, N. Wainer, K. Meier, N. Hadley, D. Soper and M. Greco, Research Directions For The Decade, Proceedings of the Summer Study, Snowmass, Colorado, page 134, World Scientific, Singapore, 1992.

[3] H.L. Lai et al. (CTEQ Collaboration), Phys. Rev. D 51 (1995) 4763.

[4] Giele, Glover and Kosower (JETRAD reference), Phys. Rev. 73 (1994) 2019.

[5] F. Abe et al. (CDF Collaboration), Fermilab preprint 96/020-E (1996).

[6] Martin, Roberts and Stirling, Phys. Lett. B 306 (1993) 145.

[7] H.L. Lai and W.K. Tung, Michigan State U. preprint, MSU-HEP-60508 or CTEQ-605 (1996).

[8] F. Abe et al. (CDF Collaboration), Phys. Rev. Lett. 77 (1996) 438.

[9] Glück, Reya and Vogt, Z. Phys. C 53 (1993) 127.

[10] I. Hinchliffe, LBNL preprint LBL-34372.

[11] S. Abachi et al. (DØ Collaboration), accepted by Phys. Rev. Lett., FERMILAB-PUB-96/072-E.

[12] H. Baer, J. Ohnemus and J. Owens, Phys. Rev. D 42 (1990) 61.

[13] F. Abe et al. (CDF Collaboration) Phys. Rev. Lett. 71 (1993) 679 and J. Alitti et al. Phys. Lett. B 236 (1991) 544.

[14] H. Baer and M.H. Reno preprint hep-ph/9603209 1 March 1996.

[15] F. Abe et al. (CDF Collaboration), Phys. Rev. Lett. 71 (1993) 680.

[16] Ya.I. Azimov, Yu.L. Dokshitzer, V.A. Khoze and S.I. Troyan, Sov. Journ. Nucl. Phys. 43 (1986) and Phys. Lett. B 165 (1985) 147; and, R.K. Ellis, G. Marchesini and B.R. Webber, Nucl. Phys. B 286 (1987) 643.

[17] F.E. Paige and S.D. Protopopescu, BNL report No. 38034 (1986).

[18] H.U. Bengtsson and T. Sjöstrand, Comp. Phys. Comm. 46 (1987) 43.

[19] G. Marchesini and B.R. Webber, Nucl. Phys. B 310 (1988) 461.

[20] L.N. Lipatov, Sov. J. Nucl. Phys. 23 (1976) 338; E.A. Kuraev, L.N. Lipatov and V.S. Fadin, Sov. Phys. JETP 44 (1976) 443; Sov. Phys. JETP 45 (1977) 199; Ya.Ya. Balitsky and L.N. Lipatov, Sov. J. Nucl. Phys. 28 822 (1978).

[21] S. Abachi et al. (DØ Collaboration), Phys. Rev. Lett. **77** (1996) 595.

[22] V. Del Duca and C.R. Schmidt, Phys. Rev. D 51 (1995) 2150; Phys. Rev. D 49 (1994) 4510.